# Sound focusing by flat acoustic lenses without negative refraction

Andreas Håkansson, Francisco Cervera, and José Sánchez-Dehesa[a)]
*Wave Phenomena Group, Nanophotonic Technology Center, Universidad Politécnica de Valencia, C/Camino de Vera s/n, E-46022 Valencia, Spain*

We present the experimental realization of two flat acoustic lenses generated by inverse design. The lenses consist of aperiodic lattices of aluminum cylinders confined in a rectangular area. They were obtained by a design tool that combines multiple scattering theory and a genetic algorithm. The cylinders' positions are optimized by the genetic algorithm in order to produce maximum sound amplification at the focal point. Both the focus and the dimension of the lenses are arbitrarily chosen. Our approach is illustrated by measurements in two lenses fabricated with aluminum cylinders 2 m long and having five and nine layers, respectively. Sound amplification up to 6.4 dB is obtained at the focus. The excellent agreement found between experimental pressure patterns and theoretical simulations supports our tool of design. It is concluded that flat acoustic lenses made of aperiodic distribution of scatterers can produce sound focusing with no need of negative refraction, a property that has been demonstrated in periodic lattices of scatterers. © *2005 American Institute of Physics*. [DOI: 10.1063/1.1852719]

The experimental demonstration of the existence of complete band gaps in two-dimensional (2D) phononic crystals (PCs)[1,2] have fueled the research in this field. At low frequencies it was demonstrated that they transmit sound at velocities lower than in air. This property combined with their low reflectance has been used to construct acoustic lenses with curved surfaces to bend the sound as the optical lenses do.[3] The properties of the acoustic lens experimentally reported were further supported by theoretical simulations.[4,5]

Recently, Yang and co-workers[6] have demonstrated that a flat acoustic lens is possible by using a closed-packed face-centered-cubic array of tungsten carbide beads embedded in water. More recently, two different groups[7,8] have predicted that acoustic imaging also can be achieved by using slabs of 2D PCs; the first one proposed a square lattice of water cylinders in mercury background,[7] the second suggested a square lattice of rigid cylinders in air.[8] This follows the observation by Hu and co-workers[9] earlier this year of the imaging effect in the propagation of liquid surface waves across a slab of copper cylinders. Some[6,7,9] of the works referred to claimed that focusing by flat lens was due to the negative refraction property[10] of the corresponding PCs. This property, which has been previously reported for their optical analogues, the photonic crystals,[11,12] allows that divergent sound beams converge without the necessity that the lens has curved surfaces. Though negative refraction is certainly expected at certain frequencies in a PCs, in our opinion, the reported claims for negative refraction behavior need a further confirmation since a simple collimation effect could also be the origin of the focusing phenomena observed. In this regard, the reader is referred to several works that appeared in the field of photonic crystals where the issue of negative refraction versus collimation effects has been previously discussed.[13,14]

In the field of photonics, focusing of light by nonconventional optical lenses has been reported by Sanchis *et al.*[15]

by using clusters of silicon cylinders in a silica background. The cylinders' positions in the cluster were determined by inverse design. In brief, the authors employed multiple scattering theory (MST) in combination with a genetic algorithm[16] (GA) that optimizes the positions of the cylinders to focus the impinging light on a prefixed focal point. Now, this procedure has been translated in the field of acoustics by Håkansson *et al.*,[17] who employed a tool of inverse design similar to the one introduce in optics[15] in order to generate acoustical lenses with nonconventional shapes.

This letter presents the experimental realization of two examples of acoustical lenses obtained by the tool of inverse design reported in Ref. 17. Though the lenses under study are not perfectly flat, the set of cylinders defining the lenses are confined in a rectangular region and, consequently, they are named "flat" and are compared with the acoustic lenses that use negative refraction to get sound focusing. Besides, here we demonstrate that focusing of sound can be obtained by aperiodic lattices of rigid cylinders in air with no need of negative refraction.

In the tool of inverse design, the two lenses here studied were generated by using the following inputs: (i) a 1700 Hz ($\lambda_0 \simeq 20$ cm) plane sound wave is considered as impinging wave. (ii) The positions of sound scatterers are restricted to occupy or to leave empty the points of a Bravais lattice with hexagonal symmetry with lattice parameter $a = 6.7$ cm. Moreover, those points are confined in a rectangular area of dimensions $127.4 \times 23.2$ and $127.4 \times 46.4$ cm$^2$, respectively. Within the defined area the lenses could contain a maximum of 39 layers of scatterers along the direction parallel to the sound wave fronts, and they are five- and and nine-layers thick, respectively, in the perpendicular direction. (iii) As scatterers we consider rigid rods of cylindrical shape, infinitely long, and with three possible diameter sizes $d$; $d = 1$, 2, and 3 cm. (iv) Finally, the focus of the lenses ($x_f, y_f$) is arbitrarily chosen at 1.2 $\lambda_0$ separated from the last layer of cylinders and placed on the acoustical axis of the lens, i.e., $x_f = 0$ and $y_f = 1.2 \lambda_0$. A GA is used to get the optimized positions and size of the cylinders that produces maximum

---

[a)]Author to whom correspondence should be addressed; electronic mail: jsdehesa@upvnet.upv.es
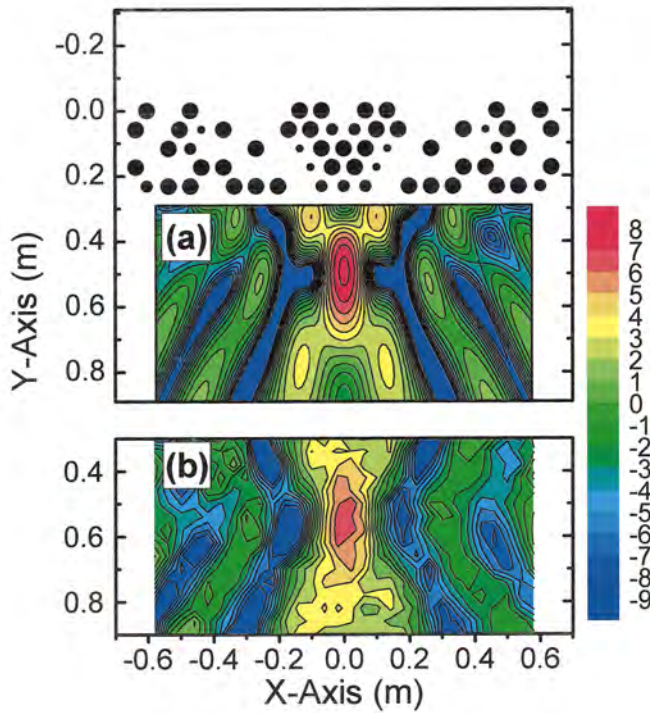
FIG. 1. (Color) Black circles define the cluster of cylinders that acts as an acoustic lens five layers thick. (a) Surface plot of the sound amplification calculated for a sound plane wave impinging on cylinders above. (b) The corresponding plot experimentally obtained.
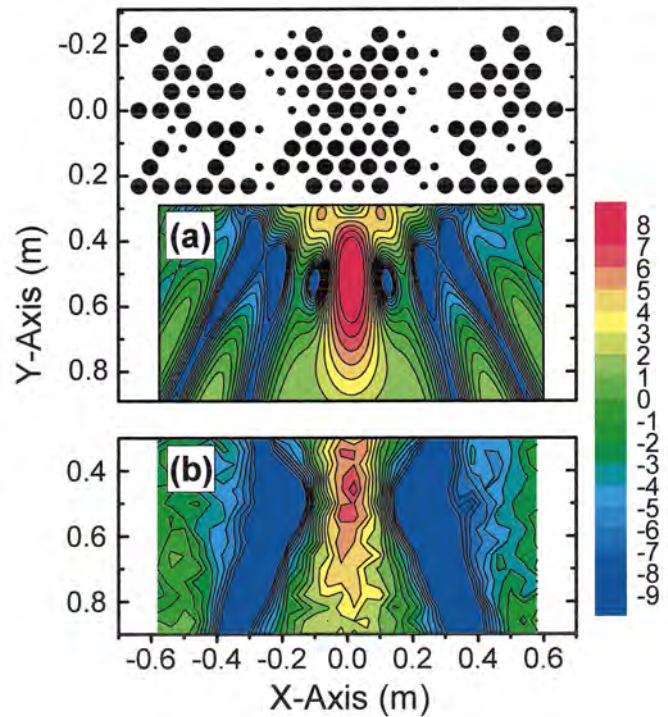


FIG. 2. (Color) Black circles define the cluster of cylinders that acts as an acoustic lens nine layers thick. (a) Surface plot of the sound amplification calculated for a sound plane wave impinging on cylinders above. (b) The corresponding plot experimentally obtained.

sound amplification at the focus, $SA_f$, which is defined as

$$SA_f(dB) = 20 \times \log_{10}\left(\frac{|P_L(x_f,y_f)|}{|P_{NL}(x_f,y_f)|}\right), \quad (1)$$

where $P_L(x_f,y_f)$ is the pressure produced by the lens, $L$, at the focal point and $P_{NL}(x_f,y_f)$ is the corresponding to the case of no-lens present. The simulation of the sound scattered by every structure analyzed by the GA is performed by a 2D MST that takes into account all the orders of multiple scattering.[18]

The top panels of Figs. 1 and 2 present the schemes of the structures of cylinders defining the lenses generated by the design tool. The size of the black circles is proportional to the rod's diameters. Surface plots of the sound amplification, $SA(x,y)$, in a restricted area behind the lens are seen in Figs. 1(a) and 2(a). Particularly, our simulations predict that the nine-layer lens achieved a larger $SA_f$ (9.98 dB) than the five-layer lens (8.35 dB) for the given incident sound plane wave. This result sounds and indicates that a larger number of scatterers should produce, in principle, an enhancement of $SA_f$.

The designed lenses are fabricated by hanging cylindrical aluminum rods (2 m long) in a frame with the corresponding hexagonal pattern. The measurements have been performed in an echo-free chamber. A white sound generated within a wide range of frequencies (from 50 to 8000 Hz) was employed as the incident sound. A collimated beam is obtained by placing the speaker at the focus of a parabolic reflector (80-cm-diam size). Pressure maps are obtained behind the lens by means of a computer controlled positioning system capable of sweeping a microphone through a grid of measuring points. Two stepped motors with a maximum resolution of 0.25 cm per step allows the movement along each $X$ and $Y$ axis. The pressure maps are obtained in a grid

of 480 points; 30 points spaced 4 cm along the $X$ axis and 16 points spaced 4 cm along the $Y$ axis. The total area scanned by the map is $116 \times 60$ cm². The rms sound pressure at each grid point, $P^{rms}(x,y)$, is automatically taken by means of a B&K 2144 frequency analyzer controlled by a GPIB interface. The microphones sample the sound with a sampling frequency of 15 kHz. The pressure spectrum with a resolution of 8 Hz is obtained by the analyzer, which makes the FFT of the data recorded by the microphone.

Figures 1(b) and 2(b) show the surface plots of the SA measured, at the working frequency of the lens $\lambda_0$. The pressure maps were measured on the equatorial plane of the lenses, i.e., at 1 m from the extremes of cylinders. In other words, experimentally, the SA at each point, $SA_{exp}(x,y)$, is determined by

$$SA_{expt}(x,y)(dB) = 20 \times \log_{10}\left(\frac{|P_L^{rms}(x,y,z=1\text{ m})|}{|P_{NL}^{rms}(x,y,z=1\text{ m})|}\right), \quad (2)$$

Both figures show that good qualitative agreement exists between the pressure maps theoretically predicted with the one measured, though the simulations are strictly 2D. A better comparison between the simulations and the measurements is shown in Fig. 3 where the SA is represented along a direction parallel to the surfaces of the lenses and that crosses the focal point. Measurements (white dots) in Fig. 3 were taken independently with an enhanced resolution, 2 cm of separation between grid points. Their comparison with the simulations above-described (dashed lines) let us to conclude that, on the one hand, sound amplification is achieved at the prefixed focus and, on the other hand, slight discrepancies are observed in the magnitude of SA and periodicity of the oscillations measured. We realized that the actual beam impinging the sample is not a plane sound wave but it is more
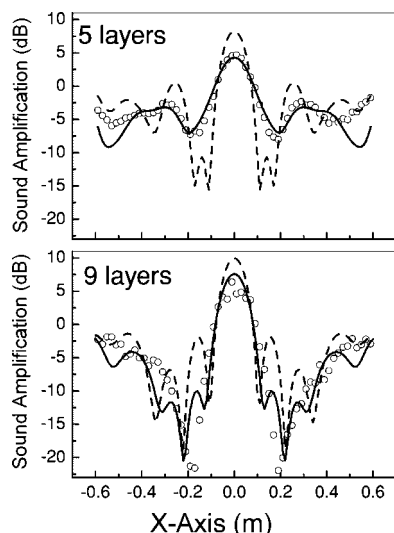
FIG. 3. Sound amplification along a direction parallel to the $Y$ axis that passes through the focal point of the lens.

similar to a Gaussian beam. Therefore, we repeated the simulations by considering a Gaussian-shape impinging beam fitted to the actual beam measured in the free-echo camera. The continuous lines in Fig. 3 represent the simulations that now show an excellent agreement with the measurements; they reproduce the periodicity of the oscillations and their amplitude. Also, the full procedure of design has been applied to the five-layer lens case by using the fitted Gaussian beam as input and no remarkable differences with the lens previously designed (see Fig. 1) have been found. This result let us to conclude the robustness of the lenses obtained by our tool of inverse design with respect to the incident beam.

The behavior of $SA_f$ with frequency for each lens is analyzed in Fig. 4. The continuous lines represent the simulations that employ a fitted Gaussian beam as impinging wave while the white dots represent the measurements. It is observed that the $SA_f$ in both lenses is spoiled when the frequency does not coincide with the working frequency of the lens $\lambda_0$. Once again, the quality of the simulations is confirmed by the excellent agreement between theory and experiment in both cases. The discrepancies observed in the
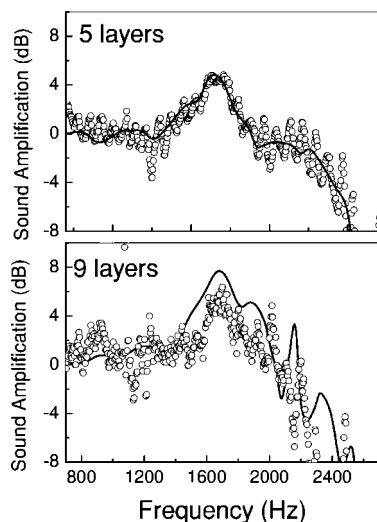
thicker lens (additional oscillations appear in the simulation) are mainly due to the fact that the actual beam does not have cylindrical symmetry with respect to the $Z$ axis and, therefore, diffused scattering is expected in this larger lens. The focal spot is ellipsoidal, its thickness (at $-6$ dB below the maximum amplification) along the $X$ axis is 20 cm ($\simeq\lambda_0$) for the five-layer lens and 13.9 cm ($\simeq 0.7\ \lambda_0$) for the nine-layer lens. At this point let us stress that we report real amplification of sound at the focal point by our lenses. Previous works[3,6] only reported sound focusing. Sound amplification at the focal point up to 4.8 and 6.4 dB has been measured in the five- and nine-layer lens, respectively.

In summary, we have demonstrated that the tool of inverse design introduced by Håkansson and co-workers[17] works well for the case of acoustic lens design in the audible range. It is important to notice that either negative refraction or collimation effects are phenomena strongly discarded in these lenses since no acoustic band formation is achieved in these aperiodic arrangements of sound scatterers. The excellent agreement obtained between theoretical simulations and experiments indicates that inverse design is a powerful tool in the field of acoustics. Its application in the range of ultrasounds is in order since it could be of enormous interest in designing new and improved ultrasonic devices.

[1] J. V. Sánchez-Pérez, D. Caballero, R. Martinez-Sala, C. Rubio, J. Sánchez-Dehesa, F. Meseguer, J. Llinares, and F. Gálvez, Phys. Rev. Lett. **80**, 5325 (1998).
[2] F. R. Montero de Espinosa, E. Jimenez, and M. Torres, Phys. Rev. Lett. **80**, 1208 (1998).
[3] F. Cervera, L. Sanchis, J. V. Sanchez-Perez, R. Martinez-Sala, C. Rubio, F. Meseguer, C. Lopez, D. Caballero, and J. Sanchez-Dehesa, Phys. Rev. Lett. **88**, 023902 (2002).
[4] B. C. Gupta and Z. Ye, Phys. Rev. E **67**, 036603 (2003).
[5] A. A. Krokhin, J. Arriaga, and L. N. Gumen, Phys. Rev. Lett. **91**, 264302 (2003).
[6] S. Yang, J. H. Page, Z. Liu, M. L. Cowan, C. T. Chan, and P. Cheng, Phys. Rev. Lett. **93**, 024301 (2004).
[7] X. Zhang and Z. Liu, Appl. Phys. Lett. **85**, 341 (2004).
[8] L.-S. Chen, C.-H. Kuo, and Z. Ye, Appl. Phys. Lett. **85**, 1072 (2004).
[9] X. Hu, Y. Shen, X. Liu, R. Fu, and J. Zi, Phys. Rev. E **69**, 030201 (2004).
[10] V. G. Vaselago, Usp. Fiz. Nauk **92**, 517 (1964) [Sov. Phys. Usp. **10**, 509 (1968)].
[11] M. Notomi, Phys. Rev. B **62**, 10696 (2002).
[12] E. Cubukun, K. Aydin, E. Ozbay, S. Foteinopoulous, and C. M. Sokoulis, Nature (London) **423**, 604 (2003).
[13] Z.-Y. Li and L.-L. Lin, Phys. Rev. B **68**, 245110 (2003).
[14] H.-T. Chien, H.-T. Tang, C.-H. Kuo, C.-C. Cheng, and Z. Ye, Phys. Rev. B **70**, 113101 (2004).
[15] L. Sanchis, A. Håkansson, D. López-Zanon, J. Bravo-Abad, and J. Sánchez-Dehesa, Appl. Phys. Lett. **84**, 4460 (2004).
[16] J. H. Holland, *Adaptation in Natural and Artificial Systems* (The University of Michigan Press, Ann Arbor, 1975).
[17] A. Håkansson, J. Sánchez-Dehesa, and L. Sanchis, Phys. Rev. B **70**, 214302 (2004).
[18] L. Sanchis, A. Hakansson, F. Cervera, and J. Sánchez-Dehesa, Phys. Rev. B **67**, 035422 (2003).

FIG. 4. Sound amplification as a function of the frequency for the two acoustic lenses under study.